CZASOPISMO TECHNICZNE M
WYDAWNICTWO POLITECHNIKI KRAKOWSKIEJ

z. 7-M/2008
ISSN 0011-4561
ISSN 1897-6328

WŁADYSŁAW MITIANIEC*, MARIAN FORMA**

# MIXTURE FORMATION AT SPRAY GUIDED DIRECT INJECTION IN SI TWO-STROKE ENGINE

# TWORZENIE MIESZANKI PRZY UKIERUNKOWANYM BEZPOŚREDNIM WTRYSKU PALIWA W SILNIKU DWUSUWOWYM ZI

Abstract

In the paper the top direct injection on the mixture formation is considered. Modelling of physics process during injection was carried out with assumption of the exact future experimental set-up. The hemisphere combustion chamber causes additional motion of gas and fuel before ignition. A difference approximation of differential equations of the injection and combustion was used for solving the problem by KIVA program. Velocity of gas influences on the distribution of liquid and vapour phases of injected fuel. In the paper: distribution of gaseous phase of fuel, gas temperature, vectors of charge velocity and vapour mass ratio for top and side fuel injection systems were shown.

*Keywords*: *combustion engines*, *crank drive*

Streszczenie

W artykule rozważano proces bezpośredniego wtrysku paliwa. Modelownie procesu fizycznego wtrysku paliwa zostało przeprowadzone przy założeniu przyszłego badawczego silnika. Półkulista komora spalania powoduje dodatkowy ruch gazu i paliwa przed zapłonem. Do rozwiązania tego problemu przeprowadzono aproksymację różnicową równań różniczkowych procesu wtrysku i spalania za pomocą programu KIVA. Prędkość gazu wpływa na rozprzestrzenianie się fazy ciekłej i parowej wtryskiwanego paliwa. W artykule pokazano rozkład par paliwa, temperaturę gazu, wektory prędkości ładunku i udział masowy par paliwa przy głowicowym i bocznym wtrysku paliwa.

*Słowa kluczowe*: *silniki spalinowe*, *wtrysk paliwa*

*Dr hab. inż. Władysław Mitianiec, Instytut Pojazdów Samochodowych i Silników Spalinowych, Wydział Mechaniczny, Politechnika Krakowska.
**Mgr inż. Marian Forma, Polski Związek Motorowy, Kraków.

## 1. Introduction

The exhaust emissions of the conventional two-stroke engine has caused increasing world-wide concerns due to environmental considerations. In the classical carburettor two--stroke engine there is a considerable short circuiting of the air fuel mixture. Direct fuel injection reduce hydrocarbon emission with proper design of the injection timing and the positioning of the injector. Location of the conventional automotive injectors should enable forming the mixture without any contact of liquid fuel with cylinder and piston walls. The overall gas flow in the two-stroke engine has a significant effect on the motion and evaporation of the fuel spray [6]. It was found that the most important parameters that strongly influence in cylinder droplet vaporisation process and spatial vapour distribution are: fluid flow pattern, injector location, injection timing and injection pressure. The evaluation of the scavenging process has an important role in the simulation process of direct fuel injection.

There is known the possibility of observations of vapour formation during injection by applying the Exciplex method used by Melton [1] or video technique for spray formation used by Ghandhi et al. [2]. However the experiments concerned to the stationary condition or very low rotational speed. New computer technique enables to observe the mixture formation after fuel injection during whole engine work cycle. Until now much work has been done in the experimental investigation of atomisation of fuel injection, but numerical modelling of such injection is relatively rare, especially for two-stroke engines. Kuo and Reitz [5] were the first who used computational model of injection and fuel droplet distribution in the cylinder. The development and simulation of the direct fuel injection needs to be based on the knowledge of the scavenging process. The two-stroke engine scavenging depends highly on the overlapping period of the exhaust port and transfer ports. The modelling in KIVA code of fuel spray and mixture formation together with gas motion during scavenge and compression process was used.

## 2. Two phase flow

Multiphase flows are characterised by two or more fluids in motion relative to each other. The fluids will also usually have different physical properties – temperature, density, conductivity. The prediction of multiphase phenomena involves computation of the values of up to 3 velocity components for each phase, 1 volume fraction for each phase and possibly: temperature, chemical composition, particle size, turbulence quantities, pressure for each phase.

Eulerian-Eulerian techniques use a fixed grid and employ the concept of 'inter-penetrating continua' to solve a complete set of equations for each phase present. The transient, convective and diffusive terms all contain the appropriate volume fraction multiplier, upwinded or averaged as required. The links between the phases – mass, momentum and heat transfer – are introduced via an interphase source. In the model the carrier fluid is the gas contained in the cylinder, which consists a residual exhaust gas and fresh air. The dispersed fluid is liquid fuel injected to the cylinder shortly before or after the exhaust port closure. The amount of fresh air with lower value of enthalpy in the cylinder than that of residual gas after scavenge process depends on the ports timing and rotational velocity.

## 3. Mathematical model of direct fuel injection

### 3.1. Exchange of phase properties

The motion of different phases of charge in the cylinder can be described by general equation

$$\frac{\partial(r_i \cdot \rho_i \cdot \varphi_i)}{\partial t} + \nabla(r_i \cdot \rho_i \cdot \mathbf{u}_i \cdot \varphi_i - r_i \cdot \Gamma_{\varphi i} \cdot \mathbf{grad}\varphi_i) = r_i \cdot S_{\varphi i} \tag{1}$$

where:

$\rho_i$ – density of phase *i*,

$\varphi_i$ – properties of phase *i* as: unitary enthalpy, unitary momentum of gas motion, mass fractions of chemical components, turbulence energy etc.,

$\mathbf{u}_i$ – velocity vector of a phase *i*,

$\Gamma_{\varphi i}$ – diffusion coefficient of φ value in the phase *i*,

$S_{\varphi i}$ – source term of exchange $\varphi_i$,

$\nabla$ – Nable's operator.

In the modelling of the injection processes and gas motion the turbulence model of Chen-Kim (κ-ε) was used [4].

### 3.2. Change of disperse phase

The basic conservation equations for modelling dispersed phase are the momentum, the mass transfer and the thermal energy transfer equations. They are briefly listed as follows

$$m_d \frac{d\mathbf{u}_d}{dt} = \mathbf{F}_{dr} + \mathbf{F}_p + \mathbf{F}_{am} + \mathbf{F}_b \tag{2}$$

Drag force $\mathbf{F}_{dr}$ is calculated from the equation

$$\mathbf{F}_{dr} = 0{,}75 \cdot C_D \cdot \rho_2 \cdot r_1 \cdot r_2 \cdot V \cdot \frac{\mathbf{u}_1 - \mathbf{u}_2}{d_d} \tag{3}$$

where:

$d_d$ – diameter of droplet,

$C_D$ – dimensionless drag coefficient given by

$$C_D = \frac{24}{\mathrm{Re}}\left(1 + 0{,}15\,\mathrm{Re}^{0{,}687}\right) + \frac{0{,}42}{1 + 4{,}25 \cdot 10^4\ \mathrm{Re}^{-1{,}16}} \quad \text{for} \quad \mathrm{Re} < 300\,000 \tag{4}$$

$V$ – cell volume.

Force operated on the droplet due to the pressure existence is described by the equation

$$\mathbf{F}_p = -V_d \cdot \nabla p \tag{5}$$

Due to the acceleration the inertia force operates on the droplet

$$\mathbf{F}_{am} = -C_{am} \cdot \rho_2 \cdot V_d \cdot \frac{d\mathbf{u}_d}{dt} \tag{6}$$

Disappearing of liquid phase of fuel due to the evaporation can be expressed as follows

$$\frac{dm_d}{dt} = -A_d \cdot K_g \cdot p_t \cdot \ln \frac{p_t - p_{v,\infty}}{p_t - p_{v,s}} \tag{7}$$

where:
$K_g$ – mass transfer coefficient,
$p_t$ – total pressure,
$p_{v,\infty}$ – partial pressure in the droplets surroundings,
$p_{v,s}$ – vapour partial pressure at the droplet surface.

During evaporation of fuel heat transfer between continuous and dispersed phases takes place based on the temperature difference as the driving force

$$m_d \frac{d}{dt}(c_{p,d} T_d) = -A_d \cdot H_d \cdot (T_d - T) + L_d \cdot \frac{dm_d}{dt} \tag{8}$$

where:
$c_{p,d}$ – droplet specific heat,
$L_d$ – latent heat of evaporation,
$H_d$ – heat transfer coefficient between droplet and gas,
$T_g$ – temperature of continuous phase,
$A_d$ – surface area of liquid droplet per unit volume, which is given by

$$A_d = \frac{6 \cdot r_2}{d_d \cdot V_{ol}} \tag{9}$$

The heat transfer coefficient is computed from the local Nusselt number based on the convective coefficient $k$

$$H_d = \frac{k \cdot Nu}{d_d} \tag{10}$$

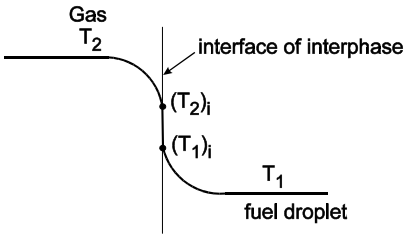


Fig. 1. Diagram of phase exchange during evaporation of liquid fuel droplets
Rys. 1. Schemat wymiany faz podczas odparowania kropli paliwa

Computation of Nusselt number is obtained from a 'fit' to the experimental data on heat transfer from spheres and is valid over the complete Reynolds and Prandtl number. Heat transfer between fuel droplet (phase 2) and gas (phase 1) trough the interface is shown in Figure 1.

### 3.3. Vapour phase

The break-up and oscillation of the fuel droplets is not taken into account in the IPSA algorithm. The initial diameter of droplets are constant and there are assumed that their

shapes are spheres. The vapour phase as third component in the charge in IPSA algorithm is calculated from the change of droplet diameter. The droplet size varies throughout the domain, as the result of evaporation. The vapour phase behaves like the disperse phase 2, but without interphase mass transfer. Then changes in droplets size can be calculated from local volume fraction ratios

$$\frac{d_d}{(d_d)_{in}} = \left(\frac{r_2}{r_s}\right)^{0,333} \tag{11}$$

The value of $r_s$ is the volume fraction of evaporated fuel and $(d_d)_{in}$ is the initial diameter of droplet.

## 4. Engine mesh generation

The engine used for the present simulation is a single cylinder two-stroke gasoline engine. The piston top was flat and the combustion chamber consists of a hemisphere. Two transfer ports are symmetric about the vertical plane crossing the axis of the cylinder and the centre of exhaust port. The generation of mesh was done by pre-processor KIVA3V and simulation was done by using recompiled version of this programme. Modelling concerned the stationary two-stroke engine Robin EC12 from Heavy Fuji Industries. During piston motion the amount of layers in *z*-axis changes causing the deformation of cells in this direction. Therefore the appropriate relaxation values were needed to fill Courant conditions especially for velocity vectors by change of time step during calculations.

The specification of the modelling two-stroke engine is given in the Table 1 and the engine mesh is shown in Fig. 2. In simulation it was assumed that the injector in the first case was located in the cylinder head and in the second case on the wall of the exhaust port enabling the fuel injection before closing of the injector port by the piston.

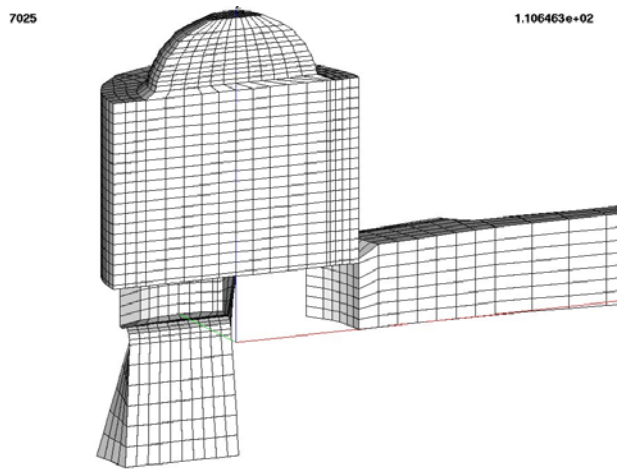


Fig. 2. Mesh of two-stroke engine Robin EC12
Rys. 2. Siatka obliczeniowa dwusuwowego silnika Robin EC12

Table 1

**Engine specification with direct fuel injection**

| | |
|---|---|
| Number of cylinder | 1 |
| Swept volume [cm$^3$] | 115 |
| Bore [mm] | 54 |
| Stroke [mm] | 50 |
| Connecting rod length [mm] | 110 |
| Compression ratio | 8 |
| Transfer ports close [°] ABDC | 57 |
| Exhaust port close [°] ABDC | 77 |

The locations of the injectors for both cases are shown in Fig. 3 and geometrical values are inserted in Tab. 2. The model enables change of the mesh during piston motion and simulation includes whole engine work cycle.

Table 2

**Injection specification**

| Injection type | X [mm] | Z[mm] | α [°] | β [°] | Start of injection BTDC [deg] | Duration of injection [deg] |
|---|---|---|---|---|---|---|
| Top injection | 12 | 63 | 10 | 60 | 95 | 35 |
| Side injection | 26 | 40 | 120 | 70 | 75 | 35 |

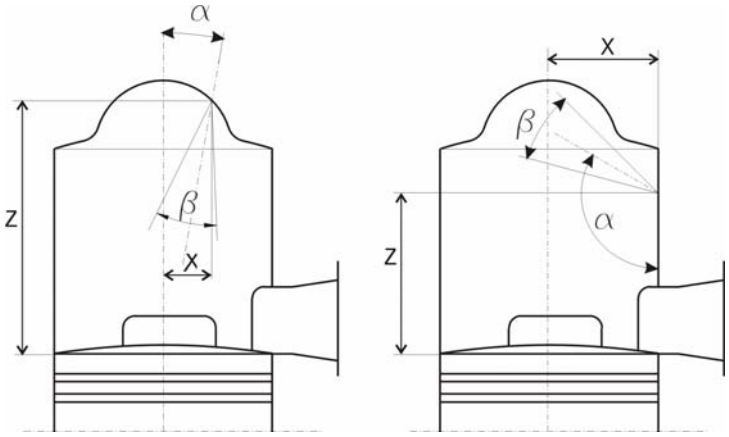


Fig. 3. Geometry of injector at top and side position
Rys. 3. Geometria usytuowania wtryskiwaczy przy głowicowym i bocznym wtrysku paliwa

## 5. Boundary and initial conditions

All the transport equations require specifications for their boundary values. The initial values were taken from experimental research and can be taken also from the numerical simulation based on zero-dimensional model. Both transfer ports had the same values of velocity and pressure but changeable in time. Variation of pressure in transfer ports and exhaust port is shown in Fig. 4.

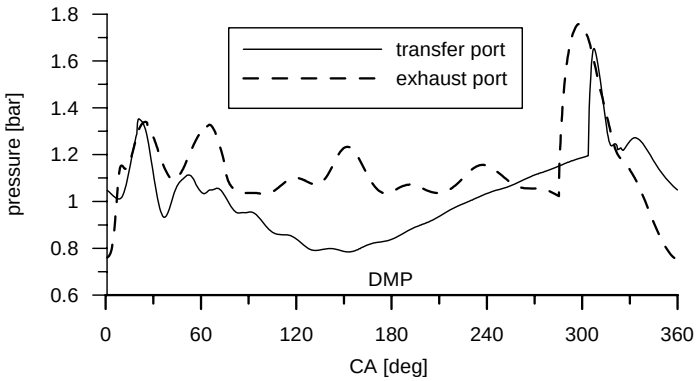


Fig. 4. Pressure in exhaust port and transfer port from experiment
Rys. 4. Ciśnienie w oknie wylotowym i przelotowym z pomiarów

The appropriate values were given in simulation programme as boundary conditions. The scalar factor for fresh charge (air) is 1,0 at the transfer port and zero for exhaust port. The cylinder walls were assumed to be smoothed and heat exchange with walls was taken into account. The k-ε turbulence model was considered and turbulence initial length scale was given as 0,001 m. The temperature of the air in transfer port was assumed as 300 K.

Simulations were carried out for whole scavenging process to obtain the initial values for simulation of fuel injection, spray and mixture formation for both injection cases. Modelling of injection process was conducted only for one rotational speed 3000 rpm, when there is enough time both for cleaning of the cylinder by fresh charge (air) during scavenging process and evaporation of injected fuel. In calculation equal initial values of fuel droplet 0,025 mm were assumed for both analyzed fuelling systems.

## 6. Calculation results

### 6.1. Scavenge process

Combustion of the injected fuel depends on local air-fuel ratio and the scavenge process has significant effect on the air distribution in the cylinder. After scavenge process in the cylinder stay much residual exhaust gas particularly at high rotational speed. However,

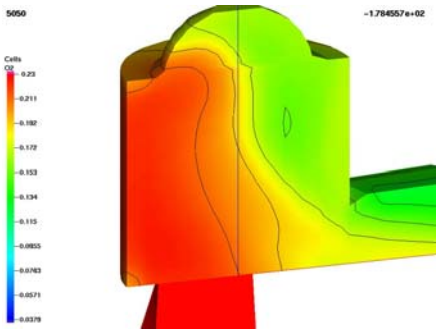


Fig. 5. Mass concentration of oxygen in the cylinder at DMP
Rys. 5. Udział masowy tlenu w cylindrze przy położeniu tłoka w DMP

much exhaust gas causes bigger temperature of the charge which helps to evaporate of injected fuel. The mass ratio of oxygen in the cylinder at BDC is shown in Fig. 5.

Most of residual gas stays near the combustion chamber and because of higher temperature has an effect on quicker evaporation of fuel. At higher speed the start of injection should be earlier in order to evaporate the fuel in the same time as for lower speed. Computational results of the DFI model provide three-dimensional information of gas flow velocities, fresh charge fraction, pressure and density distribution, turbulence as well as fuel droplet position, size, flow direction and fuel vapour fraction. The injection parameter were given as initial values: injection pressure – 20 bar, initial fuel velocity – 50 m/s and angle of injection cone – 60–70°.

### 6.2. Charge motion during fuel injection

The scavenge process and piston motion take effect on the forming of the charge motion in clock-wise direction in the combustion chamber called as "tumble". The gas motion influences on a local fuel distribution during fuel injection. Velocity vectors of continuous phase for both cases of injection are shown in Fig. 6 at 63 deg ABDC for TFI[1] and 90 deg ABDC for SFI[2]. During the fuel injection process there is an interaction of the fuel and gas in the combustion chamber, that is seen in Fig. 7 for both cases: at 90 deg BTDC for TFI and 60 deg BTDC for SFI, respectively. Fuel injection started after closing of the exhaust port.

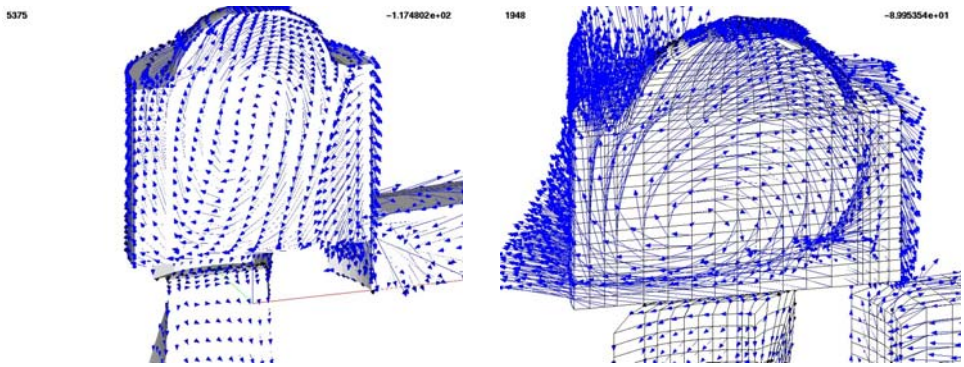


Fig. 6. Velocity vectors at 63 deg CA ABDC at TFI and 90 deg CA ABDC at SFI
Rys. 6. Wektory prędkości gazu przy położeniu tłoka 63° po DMP dla TFI i 90° po DMP dla SFI

During top injection in the cylinder the strong tumble of the charge in the parallel planes to the *z*-axis takes place and turns the fuel spray directly to the piston and causes the break of the fuel droplets. In this cases shortly before the ignition, the maximum of velocity reaches 30 m/s. During side injection the fuel velocity is decreased by the gas motion (tumble) in the combustion chamber. Compressed counter-clock-wise tumbling flow is formed, which may assist fuel droplet evaporation and also the combustion process.

[1]TFI – Top Fuel Injection.
[2]SFI – Side Fuel Injection.

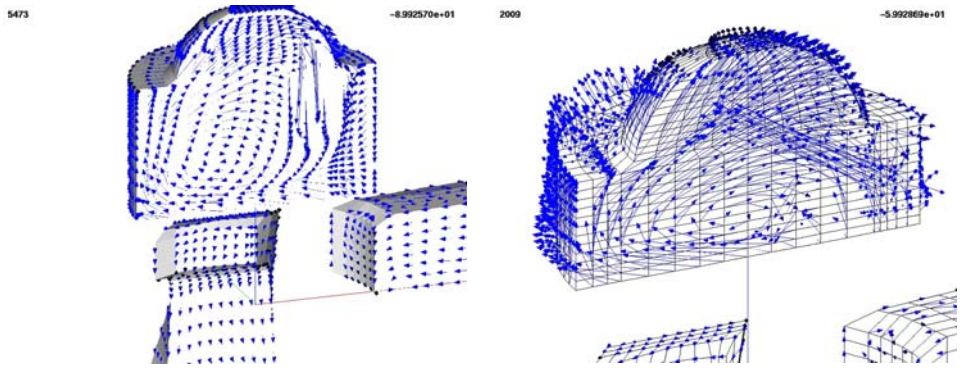


Fig. 7. Velocity vectors in the cylinder at 90 deg ABDC during TFI and at 60 deg BTDC at SFI
Rys. 7. Wektory prędkości gazu przy położeniu tłoka 90° po DMP dla TFI i 60° przed GMP dla SFI

### 6.3. Distribution of fuel gaseous phase

The slides in Fig. 8 represent the sectional contour plots of the mass fuel gaseous phase concentration of two cases. The bigger initial velocity of injected fuel causes a narrow spray in the case of top injection. The fuel vapours reach the piston crown and next the gas tumble causes their propagation in the chamber. On the other hand at side fuel injection the liquid fuel has contact only with hot air and because of high concentration in small space evaporates longer. Fig. 8 shows mass fraction of the gaseous fuel in cylinder at 83 deg CA BTDC for TFI and at 60 deg CA BTDC at SFI.

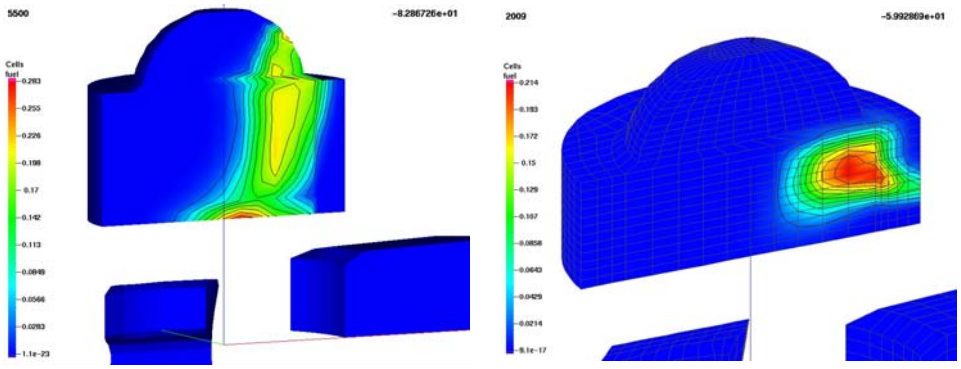


Fig. 8. Mass fraction of liquid phase at 83 deg CA BTDC at TFI and at 60 deg CA BTDC at SFI
Rys. 8. Udział masowy par paliwa przy 83° przed GMP dla TFI i przy 60° przed GMP dla SFI

Very important factor at direct fuel injection is the air-fuel ratio near the spark plug. At TFI case the mass concentration of vapours is higher at opposite side of the exhaust port and reaches air excess ratio near one ($\lambda = 1$). At side injection higher concentration of the fuel vapours is observed in the combustion chamber at side of the exhaust port, which is shown in Fig. 9. This phenomenon is caused by the gas motion, that does not enable to propagate of the fuel into the chamber. When the combustion process begins the liquid phase quickly evaporates.

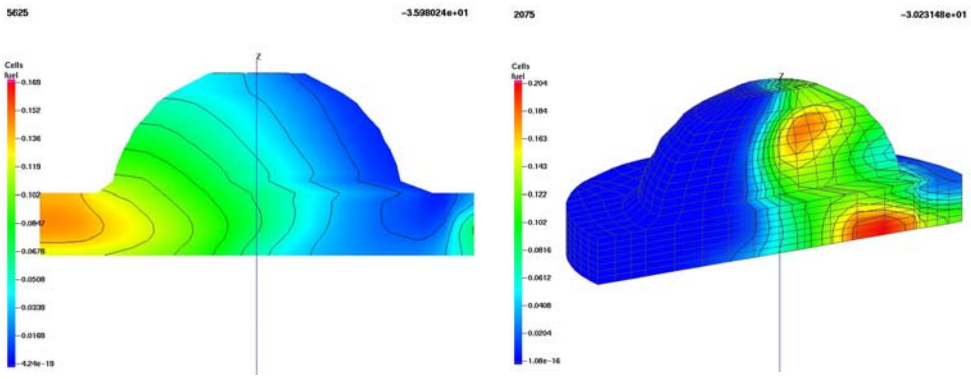

Fig. 9. Mass fraction of gaseous phase at 36 deg BTDC at TFI and at 30 deg CA BTDC at SFI
Rys. 9. Udział masowy par paliwa przy 36° przed GMP dla TFI i przy 30° przed GMP dla SFI

### 6.4. Temperature of the charge

Temperature of gas phase changes during motion of fuel spray and evaporation and its distribution inside the cylinder is different for both analysed cases (Fig. 10). Injected fuel lowers the temperature of continuous phase. Temperature distribution inside the cylinder determines the process of fuel evaporation. At top injection most of fuel evaporates quickly after leaving of the nozzle and fuel vapours reach the piston crown. Only small amount of liquid fuel stay on the piston. Fuel evaporation decreases the charge temperature about 100 K. Contrary at the side injection most of fuel evaporates in combustion chamber decreasing the temperature of gas to about 420 K at 60 deg CA BTDC. Shortly before the ignition temperature inside the cylinder is about 750 K and ignition of the air-fuel mixture depends on a local excess air ratio. The ignition for the both cases of fuel injection is shown in Fig. 11. For both cases the ignition process is successful for combustion of the air-fuel mixture causing also quick evaporation of the rest fuel droplets.

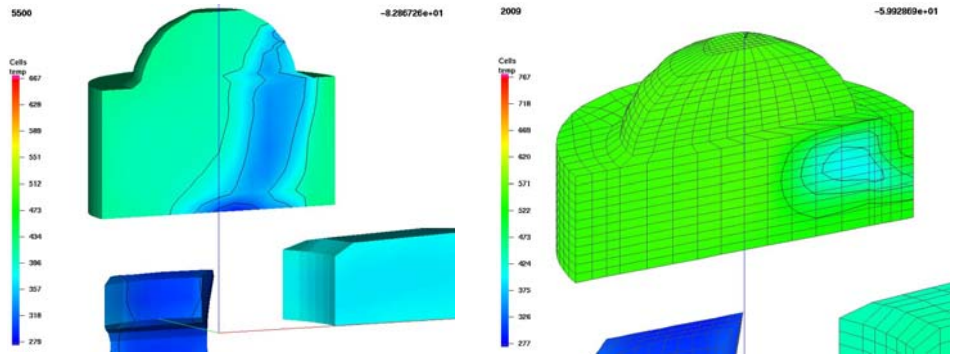

Fig. 10. Temperature in the cylinder during TFI at 83 deg CA BTDC
and during SFI at 60 CA deg BTDC
Rys. 10. Temperatura w cylindrze podczas TFI przy 83° przed GMP
i dla SFI przy 60° przed GMP

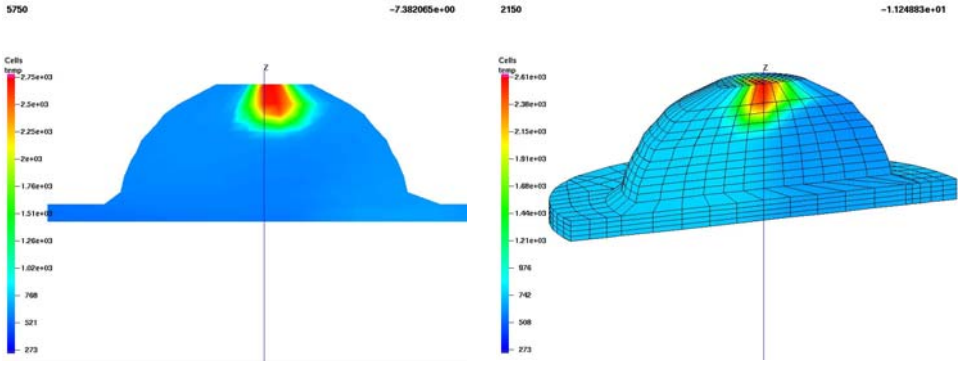

Fig. 11. Temperature in the cylinder during TFI at 7 deg AC BTDC and at 11 deg CA BTDC at SFI
Rys. 11. Temperatura w cylindrze podczas TFI przy 7° przed GMP i dla SFI przy 11° przed GMP

## 6.5. Fuel evaporation

In two-stroke engines with direct fuel injection there is a short time for fuel evaporation and it is important the mixing of air and fuel and initial temperature of the charge. Total amount of injected fuel was assumed as 0,55 g/cycle at TFI case and 0,038 g/cycle at SFI case. At TFI case the whole mass of liquid fuel evaporated fully at 60 deg CA BTDC (Fig. 12) and all fuel burned during the combustion process. At SFI case evaporation process lasted longer and small amount of fuel does not burn fully during the combustion process and is emitted to the exhaust port (Fig. 13). For the assumed initial conditions and geometrical parameters the TFI case is better for evaporation and full burning of the fuel, which is caused by the gas tumble and fuel spray guided by the air. The program KIVA calculates every time step the diameter of the droplets in whole space of the chamber.

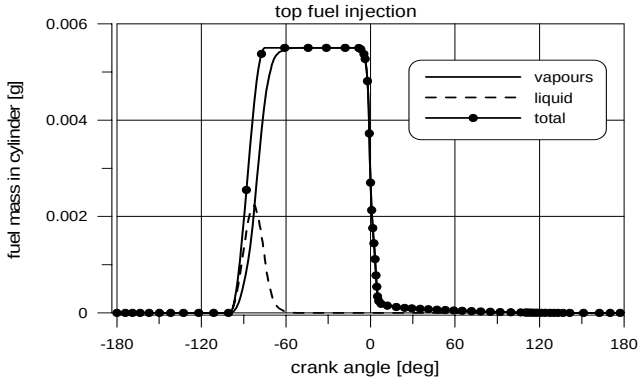


Fig. 12. Mass of liquid and vapours of fuel in cylinder at top injection
Rys. 12. Masa ciekłego i odparowanego paliwa w cylindrze przy głowicowym wtrysku paliwa

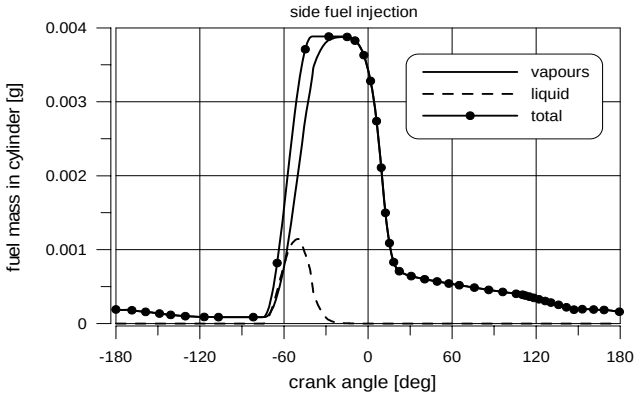


Fig. 13. Mass of liquid and vapours of fuel in cylinder at side injection
Rys. 13. Masa ciekłego i odparowanego paliwa w cylindrze przy bocznym wtrysku paliwa

## 7. Conclusions

New modern two-stroke engines and environmental protection require new fuelling systems and one of the most promising method is direct spray guided fuel injection. Many work were done in this subject, however still there is no better option for small power two--stroke engines. In this paper two possibilities of direct fuel injection were presented.

1. High pressure direct fuel injection enables to form smaller fuel droplets in the spray and quick fuel evaporation.
2. The tumble motion of the gas is favourable for fuel droplets break-up, mixing and propagation inside the combustion chamber for both considered cases: TFI and SFI.
3. With regard to the fuel evaporation and full burning the better case is top direct injection system.
4. For both cases the excess air ratio near the spark plug is enough for ignition.
5. With direct fuel injection the charge in the combustion chamber is stratified and the local air-fuel ratio changes at time, which is caused by gas tumble.
6. The real two-stroke engine with TFI system has been prepared for future investigations.

## References

[1] Melton L.A., *Exciplex-Based Vapor/Liquid Visualization Systems Appropppriate for Automotive Gasolines*, Report #1, Contract #27, Energy Research Applications Program, Texas Higher Education Coordinating Board, November, 1990.

[2] Ghandi J.B., Felton P.G., Gajdeczko B.F., Barcco F.V., *Investigation of the Fuel Distribution in a Two-Stroke Engine with an Air-Assisted Injector*, SAE Paper 940394, SAE International Congress and Exposition, Detroit 1994.

[3] Ikeda Y., Nakajima T., Kurihara N., *Spray Formation of Air-Assist Injection for Two-Stroke Engine*, SAE Paper 950271, SAE International Congress & Exposition, Detroit 1995.

[4] Chen Y.S., Kim S.W., *Computation of Turbulent Flows Using an Extended k-e turbulance closure model*, NASA CR-179204, 1987.
[5] Kuo T., Reitz R., *Three-dimensional computations of combustion in premixed-charge and direct-injected two-stroke engines*, SAE paper 920425, 1992.
[6] Mitianiec W., *Wtrysk paliwa w silnikach dwusuwowych małej mocy*, Polska Akademia Nauk, Kraków 1999.

W tekstach obcojęzycznych Redakcja dokonała tylko standardowej adiustacji, zachowując ich oryginalną wersję.